Contribution of the nucleation and recovery of disconnections to shear viscosity in diffusional creep

Francis Delannay

Université catholique de Louvain, Institute of Mechanics, Materials and Civil Engineering, iMMC/IMAP, Place Sainte Barbe 2, B-1348 Louvain-la-Neuve, Belgium, francis.delannay@uclouvain.be.

Abstract

According to the principles of diffusional creep, the normal and tangent components of the velocity jumps between adjacent grains arise from, respectively, the climbing and sliding of disconnections along grain boundaries. Stationary deformation thus implies a balance between nucleation and recovery of moving disconnections. The model considers a periodic lattice of hexagonal grains with nucleation of disconnection multipoles at triple junctions. The strain energy coupled to the population of climbing disconnections is calculated by inferring that the internal strain field associated to disconnection pile-ups brings a distribution of tractions along GBs that is consistent with the field of diffusion potential gradient that drives disconnection climb. It follows that the distribution of the density of climbing disconnections is parabolic and that the dissipation due to the nucleation and recovery of climbing disconnections is equal to 50% of the dissipation arising from diffusion fluxes. These results hold for both Nabarro-Herring creep and Coble creep. The analysis of the disconnection nucleation process highlights the sources of non-Newtonian behaviour and the existence of a threshold stress as an intrinsic feature of diffusional creep.

Keywords: diffusional creep, disconnection, nucleation, grain boundaries, climb, grain boundary sliding

Corresponding author: francis.delannay@uclouvain.be. Tél +32479738784

1. Introduction

More than seven decades ago, Nabarro and Herring brought to light the fact that diffusion fluxes from/to vacancy sources/sinks located on grain boundaries (GBs) can cause a polycrystal to deform without dislocation activity in the bulk of the grains [1, 2]. This deformation mode is commonly designated either as “Nabarro-Herring-Coble creep” or as “diffusional creep” [3-5]. The signature of diffusional creep is a large decrease of the creep resistance with decreasing grain size coupled with a stress exponent tending to 1. Diffusional creep is considered to play a major role in the sintering of porous aggregates and in the superplastic behaviour of micro- and nano-crystalline alloys. It is also believed to contribute to the rheology of finely-grained crystalline rocks in the Earth’s mantle.

The addition/removal of lattice species to/from a GB brings a velocity jump between adjacent crystals in the direction normal to the GB. As first pointed out by Lifshitz [6], diffusional creep requires concomitantly the occurrence of GB-sliding bringing a component of velocity jump in the direction parallel to the GB. It was early proposed that these two velocity jump components can be apprehended as resulting from the climb and glide of “GB-dislocations” having Burgers vector respectively perpendicular and parallel to the GB [4, 7-10]. More recent theoretical advances have elucidated the nature of such GB-dislocations by introducing the concept of disconnection [11-13]. A disconnection is a line defect on the interface between two crystalline grains which combines a dislocation character defined by a Burgers vector and a step character defined by a step height. The Burgers vector depends on the relative misorientation of the grains. Given a misorientation, it is a vector of the so-called DSC lattice which characterizes the displacement shift between the two lattices [14]. As a consequence, the average Burgers vector of the population of disconnections on GBs is smaller

than the Burgers vector of lattice dislocations (by a factor ≈ 0.2 according to Arzt et al [5]). We consider in the present paper that, during deformation, moving disconnections are dissociated into pairs of disconnections having Burgers vector perpendicular and parallel to the GB, which respectively climb and glide along GBs.

Moving disconnections disappear when reaching a triple junction (TJ) or when meeting another disconnection having opposite Burgers vector and step height. The stationary deformation of a polycrystal under a given macroscopic stress thus implies a balance between nucleation and vanishing of a density of disconnections proportional to strain rate. As this reflects the balance between strain-hardening and recovery during stationary creep, we designate the vanishing of disconnections by the term “recovery”. The internal strain energy created when disconnections nucleate dissipates when disconnections disappear. This dissipation contributes to the macroscopic shear viscosity, denoted *G*, which, for an isotropic polycrystal, is defined as

$$G = \frac{S'_{ij}}{2\dot{E}_{ij}} \tag{1}$$

where S'_{ij} and $\dot{E}_{ij}$ denote the components with $i \neq j$ of, respectively, the macroscopic deviatoric stress and the macroscopic strain rate. The present paper aims at assessing the current assumption that the contribution to *G* arising from the nucleation and recovery of the linear defects (disconnections or GB-dislocations) involved in the diffusional deformation mechanism is negligible with respect to the contribution due to diffusion fluxes.

The analysis is carried out in Section 2 for the case of a columnar monoatomic polycrystal modelled as a periodic lattice of hexagonal grains with isotropic material properties. TJs are considered to be the sole disconnection nucleation sites. The strain energy arising from

the population of climbing disconnections is calculated by inferring that the internal strain field associated to the disconnections brings a distribution of tractions along the GBs that is consistent with the field of potential gradient driving disconnection climb. The contribution to *G* due to this strain energy is found to amount to 50% of the contribution due to diffusion fluxes. The outcomes are discussed in Section 3 with reference to the various contributions to *G* that have been brought out in the literature. The existence of a threshold stress as an intrinsic feature of the diffusional creep mechanism is highlighted.

2. Contributions to dissipation

2.1. Nucleation, recovery, and pile-up of disconnections

We define the diffusion flux in the bulk of a grain, denoted **J**, as the volume of lattice atoms transported per unit surface and per unit time. **J** is driven by the gradient of the diffusion potential, denoted $\boldsymbol{\mu} = \boldsymbol{\mu}_{atom} - \boldsymbol{\mu}_V$ where $\boldsymbol{\mu}_{atom}$ and $\boldsymbol{\mu}_V$ denote the chemical potential of atom and vacancy. If material properties are considered isotropic, **J** writes [2, 15]

$$\mathbf{J} = -\frac{D_{bulk}}{kT}\nabla\left(\boldsymbol{\mu}_{atom} - \boldsymbol{\mu}_V\right) = -\frac{D_{bulk}}{kT}\nabla\boldsymbol{\mu} \tag{2}$$

where D_{bulk} is the diffusion coefficient in the bulk of the grain, *k* is Boltzman's constant, and *T* is the absolute temperature. The diffusional creep model assumes that the vacancy sources and sinks are located only on GBs, which implies that the divergence of $\mathbf{J}$ is null in the grain interior, i.e. density is uniform and $\boldsymbol{\mu}$ is harmonic. Owing to the lattice distortions around GB defects and to the internal stresses associated to the latter, the diffusion coefficient is larger close to GBs than in the bulk of the grains [16]. This feature is commonly modelled by assuming the existence of a GB-layer of thickness δ inside which the average diffusion coefficient, D_{gbl}, is larger than in the bulk [17]. Inside this layer, diffusion fluxes parallel to the GB, denoted *j*, are

defined in units of volume per unit length per unit time. As δ is small, $\boldsymbol{\mu}$ inside the GB-layer is very close to the diffusion potential on the GB, $\boldsymbol{\mu}_{gb}$, and, based on Eq. (2),

$$j = -\frac{\delta D_{gbl}}{kT}\nabla_s \boldsymbol{\mu}_{gb} \tag{3}$$

where ∇_s denotes the gradient operator on the GB surface. Taking the radius, R_G, of the equivalent sphere as measure of the average grain size, bulk diffusion is dominant when $\frac{\delta D_{gbl}}{R_G} << D_{bulk}$ (Nabarro-Herring creep), and GB-layer diffusion is dominant when $\frac{\delta D_{gbl}}{R_G} >> D_{bulk}$ (Coble creep).

As represented in Figure 1, we consider a purely deviatoric macroscopic strain rate with principal tensile direction of amplitude $\dot{E}$ oriented at an angle α with respect to the normal to one of the grain faces. We limit the analysis to small deformation: the distance 2*B* between the TJs at the ends of a GB is thus taken to remain constant during deformation. We also limit ourselves to quasi-steady-state with flat GBs: the GB curvature induced by strain rate is thus neglected [18]. Grain faces are designated by subscripts $1 \le f \le 6$, which are taken to increase anticlockwise, with faces *f* = 3 and *f* = 6 horizontal. M_f designates the middle of face *f* and, for each face, a Cartesian coordinate system with origin at M_f is defined by unit vectors ($\mathbf{x}_f$, $\mathbf{z}_f$), with $\mathbf{z}_f$ oriented outward and $\mathbf{x}_f$ defined positive anticlockwise. The direction of GB sliding, i.e. the direction of the Burgers vector of the disconnections of which glide is activated, is thus parallel to $\mathbf{x}_f$. The deformation of a periodic lattice of grains being affine by definition, the velocity jump at GBs, $\Delta\dot{\mathbf{u}}$, is linked to the macroscopic strain rate tensor, $\dot{\mathbf{E}}$, via

$$\Delta\dot{u}_i = \dot{E}_{ij}R_j \tag{4}$$

where R_j denotes the components of the vector joining the centroids of the two grains sharing the GB. It follows from variational principles that the hypothesis of affine deformation brings only an upper bound for the power dissipated during the deformation of a random polycrystal. This upper bound is nevertheless realistic because, within the limits of small deformation, the departure from periodicity does not bring the average velocity field to differ very much from the affine approximation [19]. Via Eq.(4), the normal and tangent components of the velocity jumps at the six GBs express

$$\Delta\dot{u}_{z_f} \equiv \Delta\dot{u}_{n_f} = 2\sqrt{3}B\dot{E}\cos\left(2\alpha - 2f\frac{\pi}{3}\right) \tag{5}$$

and $$\Delta\dot{u}_{x_f} \equiv \Delta\dot{u}_{//_f} = 2\sqrt{3}B\dot{E}\sin\left(2\alpha - 2f\frac{\pi}{3}\right) \tag{6}$$

$\Delta\dot{u}_{n_f}$ and $\Delta\dot{u}_{//_f}$ do thus not depend on coordinate *x*.

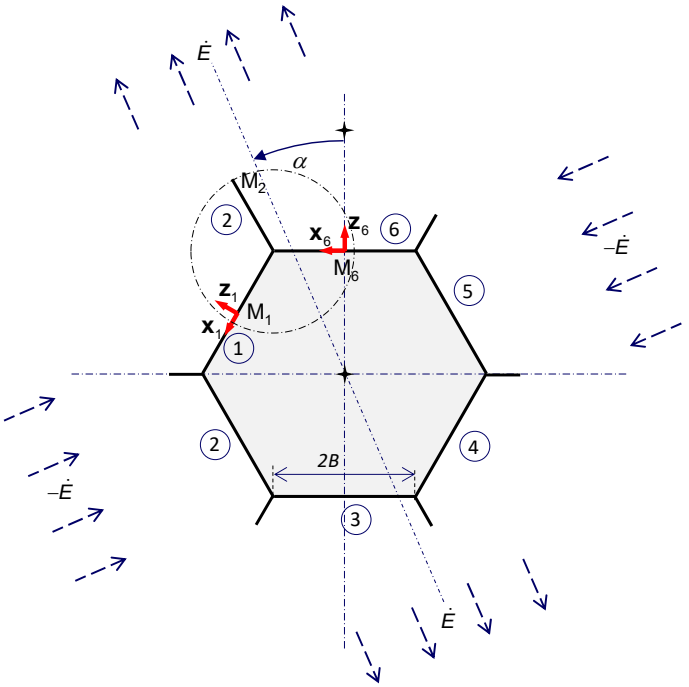

Figure 1 : Geometrical parameters of the model

Figures 2a and 2b represent magnified views of the region circumscribed by the dash-dotted circle in Fig. 1 for the orientations $\alpha = 0$ and $\alpha = \frac{\pi}{4}$. We anticipate that TJs are the most favourable locations for the nucleation the moving disconnections and we assume that the latter dissociate into pairs having Burgers vector perpendicular and parallel to the GB. A few such disconnections are depicted in red and in light-blue, respectively. Arrows drawn in red and in light-blue indicate their directions of motion. The velocity jumps components $\Delta\dot{u}_{n_f}$ and $\Delta\dot{u}_{//_f}$ result from the motion in opposite directions of disconnections of opposite sign that nucleate at opposite TJs and annihilate when meeting at GB middle (localized at M_1, M_2, and M_6). In the following, subscripts cl and gl are used for referring to climbing and gliding disconnections, respectively (subscripts *f*, cl and gl will be dropped when the distinction is not needed). In the interval $0 \le x \le B$, $\Delta\dot{u}_n$ and $\Delta\dot{u}_{//}$ may thus be expressed as

$$\Delta\dot{u}_n = \rho_{cl}(x)\dot{a}_{cl}(x)b_{cl}(x) \tag{7}$$

and

$$\Delta\dot{u}_{//} = \rho_{gl}(x)\dot{a}_{gl}(x)b_{gl}(x) \tag{8}$$

where $\rho(x)$, $\dot{a}(x)$, and $b(x)$ denote the value at x of, respectively, the density of moving disconnections (defined as length per unit surface area), their average velocity (defined as $\dot{a} = -\frac{dx}{dt}$), and the average length of their Burgers vector (with sign defined to be the same as the sign of $\Delta\dot{u}_n$ or $\Delta\dot{u}_{//}$). Burgers vectors, b_{cl_f} and b_{gl_f}, are thus uniform for $0 \le x \le B$, and, according to Eqs (5) to (8), it follows that the product $\rho_{cl}(x)\dot{a}_{cl}(x)$ or $\rho_{gl}(x)\dot{a}_{gl}(x)$ is uniform. $\rho(x)\dot{a}(x)$ is the rate of nucleation at the TJ. Fig. 2 illustrates the dependence of the nucleation phenomenon on loading orientation. When $\alpha = 0$, nucleation involves the creation of a multipole of disconnections that assembles three climbing disconnections and two sliding

disconnections. When $\alpha = \frac{\pi}{4}$, the multipole assembles two climbing disconnections and three sliding disconnections. For a general orientation of the TJ, the multipole would assemble six disconnections. The compatibility of the velocity jumps for the three GBs imposes that disconnections forming the multipole are such that both the sum of their Burgers vectors and the sum of their step heights are null.

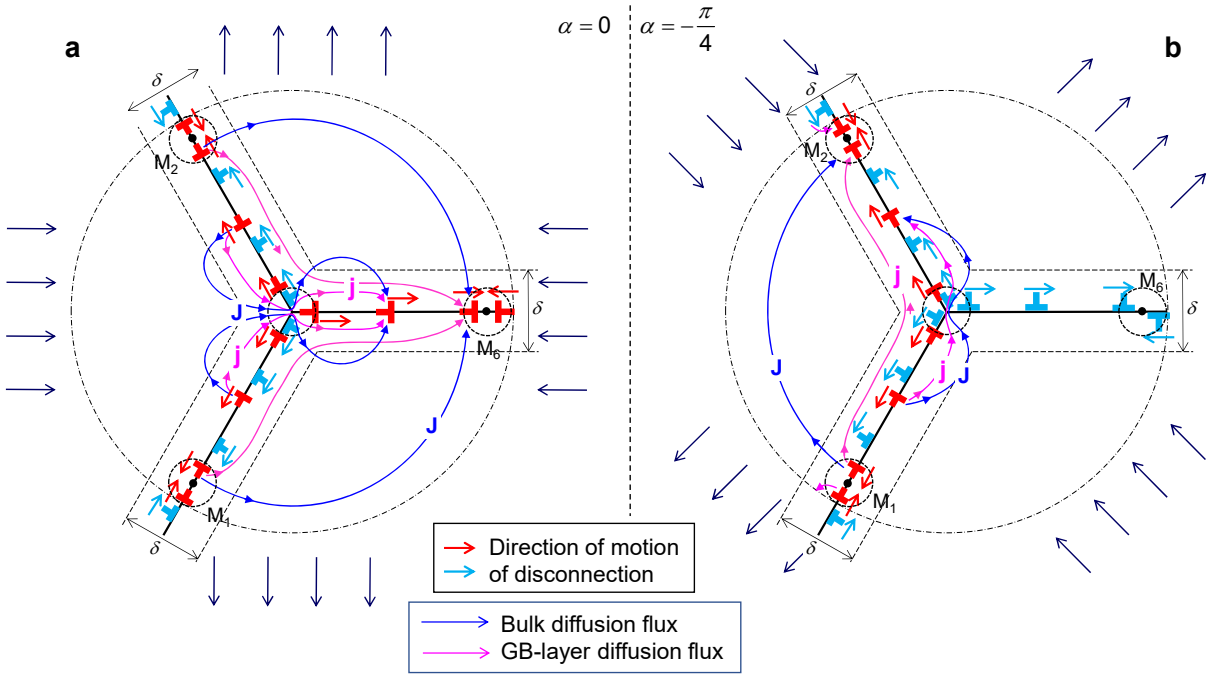

Figure 2: Region circumscribed by the dash-dotted circle in Fig. 1 for $\alpha = 0$ and $\alpha = \frac{\pi}{4}$. Red and light-blue arrows indicate the directions of disconnection motion. Trajectories of bulk diffusion fluxes are drawn in dark blue whereas trajectories of GB-layer fluxes are drawn in magenta.

GBs also contain disconnections related to the five degrees of freedom that characterise the crystallography of a GB [14]. These disconnections, which we will call "geometrical disconnections", form a population of which the density remains the same under strain rate as at rest. It is supposed that the presence of these geometrical disconnections does not affect the mobility of moving disconnections.

In conditions of Nabarro-Herring creep, disconnection climb (Eq. (7)) is fed by the sum of the components normal to the GB of the bulk fluxes, **J**, on the two sides of the GB. The field of $\boldsymbol{\mu}$ is then obtained (to a constant) by solving the Laplace equation $\nabla^2\boldsymbol{\mu} = 0$ with the boundary conditions defined by $\Delta\dot{u}_n$ (Eq. (5)). The solving of the problem is easier in conditions of Coble creep because $\Delta\dot{u}_n$ is then equal to the opposite of the divergence of *j*: the distribution $\boldsymbol{\mu}_{\mathrm{gb}}(x)$ can then be obtained (to a constant) without having to solve the Laplace equation. For the hexagonal lattice model, there exist exact solutions (i.e. solutions complying with force equilibrium) both for the case of Coble creep [20, 21] and for the case of Nabarro-Herring creep [22]. In Fig. 2, trajectories of bulk diffusion fluxes, **J**, are drawn in dark blue whereas trajectories of GB-layer fluxes, denoted **j**, are drawn in magenta. These trajectories are consistent with the fields of $\boldsymbol{\mu}$ reported in the literature [21, 22]. As GBs are assumed to be flat, the transfer of diffusion fluxes from one grain to the other occurs only through the core of the TJ [18].

The work required for the nucleation of a multipole converts into an increase of the strain energy in the polycrystal. The strain energy is released as dissipation when opposite disconnections meet at GB middle. In Fig. 2, the dotted circles drawn around the TJ and around the GB middles represent the volumes inside which strain energy increases or decreases during the events of multipole nucleation or dipole recombination. Two types of forces operate on a disconnection inside the multipole nucleation volume: (1) forces opposing the escape of the disconnection from the multipole (because the sum of the Burgers vectors of the other disconnections is opposite); (2) forces opposing the motion of the disconnection toward the preceding disconnection in the array ahead along the GB (because the Burgers vector is the same). The same two types of forces operate with opposite sign inside the dipole

recombination volume. The forces of type (1) are responsible for the dissipation associated to the nucleation/annihilation of isolated disconnections: the corresponding work power dissipated on one single GB (i.e. for $-B \le x \le B$) is denoted $\dot{W}^{isol}$. The forces of type (2) bring the array to behave as a pile-up of disconnections in which the density distribution is such that the overall strain energy is minimum. The work power dissipated on one GB due to the strain energy associated to the two pile-ups moving in opposite directions is denoted $\dot{W}^{pile-up}$.

Disconnections are isolated if the rate of nucleation is lower than $\frac{\langle \dot{a}(x) \rangle}{B}$, i.e. if $\rho \le \frac{1}{B}$. An upper bound for $\dot{W}^{isol}$ can be calculated by considering that a disconnection moving along the GB segment $0 \le x \le B$ interacts with two image forces at $x = 0$ and $x = B$: based on the classical theory of dislocations [23], one obtains for one GB

$$\dot{W}^{isol} = \frac{\Delta\dot{u}}{b} \frac{1}{4\pi} \frac{\mu}{1-\nu} L b^2 \ln\left(\frac{B}{2|b|}\right) = \frac{1}{4\pi} \frac{\mu}{1-\nu} L b \Delta\dot{u} \ln\left(\frac{B}{2|b|}\right) \quad (9)$$

where μ, ν, and L denote, respectively, the elastic shear modulus, the Poisson ratio, and the transverse depth of the columnar polycrystal, whereas $\Delta\dot{u}$ stands for either $\Delta\dot{u}_n$ or $\Delta\dot{u}_{//}$ ($\dot{W}^{isol}$ is positive because the signs of b is the same as the sign of $\Delta\dot{u}_n$ by definition). As $b_{cl} \cong b_{gl}$ on average, $\dot{W}^{isol}$ is similar for climbing and sliding disconnections. The accuracy of Eq. (9) will be discussed in Section 3.5.

If the moving disconnections form a pile-up in which they interact with one another, $\dot{W}^{pile-up}$ can be calculated via the same method as for calculating the dislocation density distribution and the force on the leading dislocation in a (static) pile-up of dislocations [23]. The array of discrete disconnections is assimilated to a continuous density, $\rho(x)$, of

disconnections with infinitesimal Burgers vectors. If grain size is large enough, the difference with respect to the discrete array is significant only over a distance from the GB equal to the discrete disconnection spacing. Beyond this distance, the stress field, $\boldsymbol{\sigma}(x, z)$, is linear elastic and, at each point on the GB, a traction vector, **T**, may be then defined, which derives from the stress tensor via Cauchy's law:

$$T_i = \sigma_{ij} n_j \tag{10}$$

where **n** denotes a unit vector normal to the GB and summation over repeated indices is implied. Sections 2.2. and 2.3 analyse successively the cases of pile-ups of climbing disconnections and pile-ups of sliding disconnections.

2.2. Pile-ups of climbing disconnections

When an atom is transferred from the interior of a grain to a sink on a GB, the diffusion potential is decreased by the work involved in the transfer [2]. If the stress field is continuous, the work amounts to $-\Omega T_n$ where $T_n = \mathbf{T} \cdot \mathbf{n}$ is the normal component of traction and Ω is the atom volume. It follows that, at the position of the core of a climbing disconnection, the diffusion potential on the GB, $\boldsymbol{\mu}_{gb}$, may be expressed as

$$\boldsymbol{\mu}_{gb} = \boldsymbol{\mu}^{\circ} + \beta W_{cl}^{nucl} - \Omega T_n \tag{11}$$

where $\boldsymbol{\mu}^{\circ}$ is a reference potential for the system at rest, W_{cl}^{nucl} denotes the strain energy coupled to the population of climbing disconnections in one single GB (i.e. either W_{cl}^{isol} or $W_{cl}^{pile-up}$), and βW_{cl}^{nucl} is the nucleation work per atom, with factor β left non specified. The assumption of a continuous disconnection density allows Eq. (11) to be valid everywhere on GBs: GBs are then said to act as perfect sources and sinks for vacancies [9]. The case of a discrete, non-continuous distribution of sources and sinks has been analysed by Arzt et al [5].

As we assume a monoatomic polycrystal, $\boldsymbol{\mu}_{gb}$ is not affected by solutes or precipitates which may cause a drag effect or a threshold stress hindering disconnection motion [5, 9].

For the disconnections located outside the nucleation or recombination volumes (Fig. 2), although the strain energy density varies along the GB, W_{cl}^{nucl} is not affected by the motion of individual disconnections because the relative position of the disconnections evolves in such a way as to keep the total strain energy minimum. It then follows from Eq. (11)

$$\nabla_s T_n = -\frac{1}{\Omega}\nabla_s \boldsymbol{\mu}_{gb} \tag{12}$$

which allows deriving the distribution of $\nabla_s T_n$ from the field of $\boldsymbol{\mu}$ calculated either via the solution of the Laplace equation, $\nabla^2 \boldsymbol{\mu} = 0$, or via Eq. (3). For the disconnections inside the nucleation/recombination volumes, the gradient of W_{cl}^{nucl} is large and Eq. (12) is not valid. Moreover, T_n cannot be defined inside these volumes because, as the scale is similar to the discrete disconnection spacing, the stress field derived from the continuous density approximation breaks down. Nevertheless, as the continuity of the diffusion potential imposes that $\boldsymbol{\mu}_{gb} = \boldsymbol{\mu}^{\circ}$ at TJs, a traction offset, $T_n^{nucl} = \frac{\beta}{\Omega} W_{cl}^{nucl}$, may be defined such that T_n tends to T_n^{nucl} at TJs: the classical assumption in the literature that T_n tends to zero at TJs implicitly involves the approximation that the nucleation work is null.

In the case of Coble creep, Eqs (3) and (12) yield for each grain face

$$\frac{dT_{n_f}^{Coble}}{dx_f} = \frac{kT}{\Omega\delta D_{gbl}} j_f = -\frac{kT}{\Omega\delta D_{gbl}} \Delta\dot{u}_{n_f} x_f . \tag{13}$$

The distribution $T_n^{Coble}(x)$ is thus parabolic with an extremum at $x = 0$. In the case of Nabarro-Herring creep, $\boldsymbol{\mu}_{gb}$ is also parabolic (as early pointed out by Lifshitz [6] and Beere [24]): based

on the solution calculated by Rudge [22], Eqs (2) and (11) yield

$$\frac{dT_{n_f}^{NH}}{dx_f} = -\frac{2}{\sqrt{3}}\frac{1}{B}\frac{kT}{\Omega D_{bulk}}\Delta\dot{u}_{n_f} x_f . \tag{14}$$

In the following, Eqs. (13) and (14) are lumped in the form

$$\frac{dT_n}{dx} = -A\Delta\dot{u}_n x. \tag{15}$$

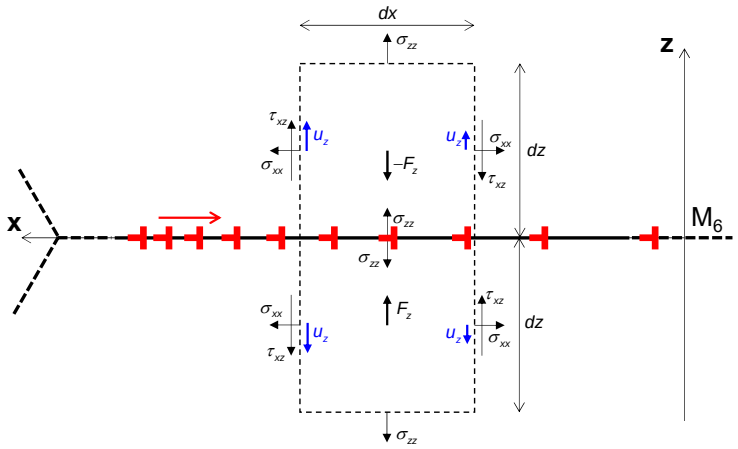

Figure 3: Static equilibrium of adjacent volume elements on the two sides of a GB

The distribution of the density of climbing disconnections can be calculated by inferring that the gradient of diffusion potential driving climbing has to be consistent with the internal stress field due to the pile-up [25]. For this purpose, Figure 3 depicts the static equilibrium of adjacent volume elements on the two sides of the horizontal GB represented in Fig. 2a. On the one hand, the fact that $\frac{dT_n}{dx} \neq 0$ implies the existence of body forces per unit volume, denoted $\pm F_z$, which oppose one another:

$$F_z = \frac{dT_n}{dx} = \frac{\partial \sigma_{zz}}{\partial x}. \tag{16}$$

On the other hand, as $\frac{\partial \sigma_{zz}}{\partial z} = 0$ by symmetry, it follows from force equilibrium that

$$-F_z = \frac{\partial \tau_{xz}}{\partial x} = \mu \frac{\partial^2 u_z}{\partial x^2} \tag{17}$$

where μ denotes the elastic shear modulus and u_z denotes the *z* component of the displacement (Fig. 3). The density of climbing disconnections brings a gradient of displacement

$$\frac{du_z}{dx} = -\frac{1}{2} b_{cl} \rho_{cl}. \tag{18}$$

Eqs (15) to (18) yield

$$\frac{d\rho_{cl}}{dx} = -2\frac{1}{\mu b_{cl}} \frac{dT_n}{dx} = 2A \frac{1}{\mu b_{cl}} \Delta \dot{u}_n x, \tag{19}$$

i.e., as $\left(\rho_{cl}\right)_{x=0} = 0$,

$$\rho_{cl} = A \frac{1}{\mu b_{cl}} \Delta \dot{u}_n x^2. \tag{20}$$

The distribution of the density of climbing disconnections need thus to be parabolic. By coupling Eq. (20) with Eq. (7), the climbing velocity is obtained as

$$\dot{a}_{cl} = \frac{\mu}{A} \frac{1}{x^2}. \tag{21}$$

$\dot{a}_{cl}$ depends neither on the velocity jump, nor on the disconnection Burgers vector and tends to the infinite as x^{-2} for the disconnection approaching the GB middle. Incidentally, it may be mentioned that the uniformly distributed array of GB-dislocations assumed by Arzt et al [5] is not consistent with the gradient of diffusion potential driving the climbing of the array (an array of equally spaced identical dislocations creates a disclination [25]).

From Eqs. (18) and (20), the variation along the GB of the total displacement $\Delta u_z = 2\|u_z\|$ is obtained as

$$\Delta u_z = \frac{1}{3} A \frac{1}{\mu} \Delta \dot{u}_n \|x\|^3. \tag{22}$$

The average of Δu_z is

$$\left\langle \Delta u_z \right\rangle = \frac{1}{B}\int_0^B \Delta u_z dx = \frac{1}{12}B^3 A \frac{1}{\mu}\Delta \dot{u}_n = \frac{1}{4}\left(\Delta u_z\right)_{x=B}. \tag{23}$$

The strain energy associated to the double pile-up in one single GB, $W_{cl}^{pile-up}$, may be calculated by assimilating each pile-up to a crack [23]. Assuming a linear elastic behaviour, the work to be spent for creating two cracks with tip at $x = 0$ having an opening distribution $\Delta u_z(x)$ and a traction distribution on the faces $T_n(x)$ writes

$$W_{cl}^{pile-up} = \frac{1}{2}L\int_{-B}^{B}\left(T_{n0} - T_n\right)\Delta u_z dx \tag{24}$$

where T_{n0} denotes the traction at $x = 0$. According to Eqs (15) and (22), the strain energy density per unit GB surface area, $\left(T_{n0} - T_n\right)\Delta u_z$, varies as x^5. Via Eq (23), Eq. (24) yields

$$W_{cl}^{pile-up} = \frac{1}{3}ALB^3 \Delta \dot{u}_n \left\langle \Delta u_z \right\rangle. \tag{25}$$

As $\frac{d\left\langle \Delta u_z \right\rangle}{dt} = \Delta \dot{u}_n$, the work power needed for the maintenance of two stationary pile-ups is

$$\dot{W}_{cl}^{pile-up} = \frac{1}{3}ALB^3 \Delta \dot{u}_n^2. \tag{26}$$

Eq. (26) is valid only when the disconnection density may be approximated as continuous (otherwise, Eq. (11) is not valid): at low strain rate, the work power for nucleation tends to $\dot{W}_{cl}^{isol}$ (Eq. (9). If $\dot{W}_{cl}^{pile-up} >> \dot{W}_{cl}^{isol}$, the traction offset, T_n^{nucl}, toward which T_n tends at TJs is derived as

$$T_n^{nucl} = \frac{\dot{W}_{cl}^{pile-up}}{2BL\Delta \dot{u}_n} = \frac{1}{6}AB^2 \Delta \dot{u}_n. \tag{27}$$

It then follows from Eq. (15), that the normal traction distribution writes

$$T_n = \frac{1}{2} A \Delta \dot{u}_n \left(\frac{4}{3} B^2 - x^2 \right) \tag{28}$$

Figure 4 presents the distributions $T_{n_f}(x)$ expressed by Eq. (28) with $\Delta \dot{u}_{n_f}$ given in Eq. (5) for the same loading orientations as in Fig. 2. The curves are dashed inside the volumes of nucleation and recombination because, strictly speaking, T_n cannot be calculated inside these volumes. The magnitude of the nucleation work at TJs is figured by the stress offset, T_n^{nucl}, at TJs.

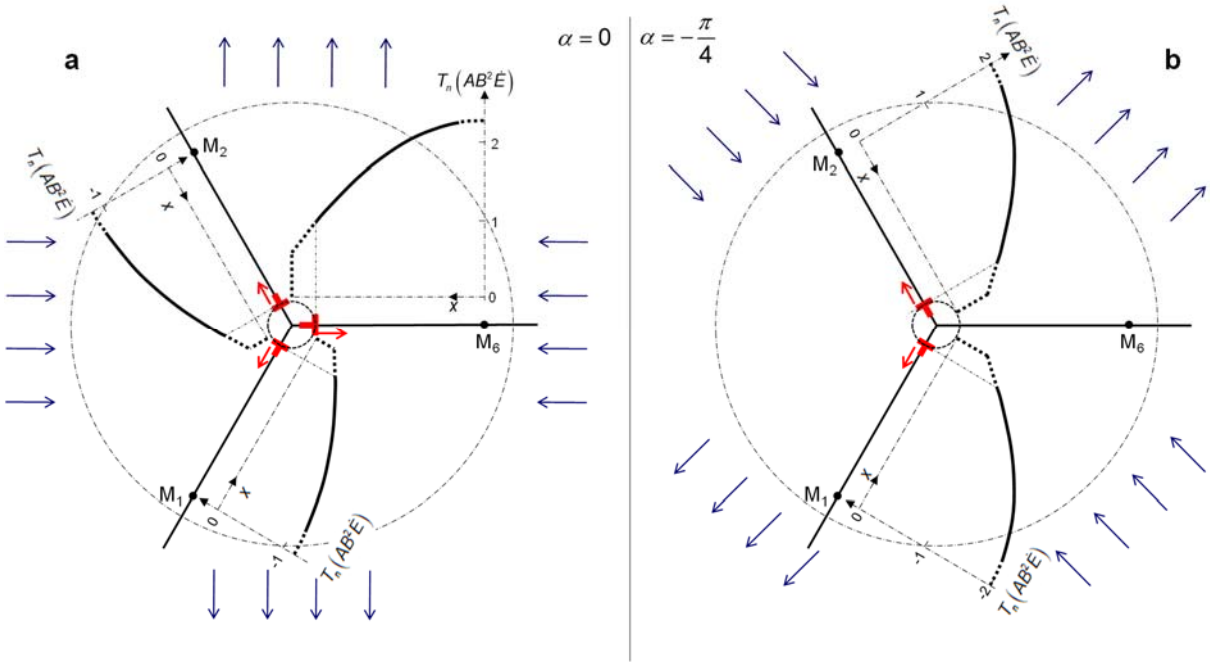

Figure 4: Distributions $T_{n_f}(x)$ for the same loading orientations as in Fig. 2.

2.3. Gliding disconnections

The mechanical equilibrium of a pile-up of gliding disconnections can be analysed in a similar manner as depicted in Fig. 3 for the case of climbing disconnections. The only difference is that a gradient of the tangent component of the traction vector, $T_{//}$, then results from body forces per unit volume parallel to the GB. Following Lifshitz [6], it is widely admitted that the

resistance against grain boundary sliding may be modelled via a linear relationship between $T_{//}$ and the tangent velocity jump, $\Delta\dot{u}_{//}$, in the form

$$\Delta\dot{u}_{//} = \frac{1}{\eta} T_{//} \tag{29}$$

where η is a parameter called by Lifshitz "grain boundary viscosity". As $\Delta\dot{u}_{//}$ is uniform (Eq.(6)), Eq. (29) implies that $T_{//}$ is uniform. Based on Eqs (16) to (20), it follows that $\rho_{gl} = 0$ and $\dot{W}_{gl}^{pile-up} = 0$: gliding disconnections do thus not interact with one another. The fact that ρ_{gl} tends to zero means that the gliding velocity $\dot{a}_{gl}$ tends to the infinite. The large difference between $\dot{a}_{cl}$ and $\dot{a}_{gl}$ reflects the fact that, whereas disconnection climb requires long range displacements by diffusion, disconnection glide requires only shuffling displacements of lattice constituents to overcome Peierls barriers. When both climbing and sliding disconnections move simultaneously along a GB, they may be considered as belonging to distinct, non-interacting arrays moving at very different velocities.

3. Discussion

Models for creep are usually assessed by comparison with experimental measurements of the quasi-stationary creep rate under uniaxial loading. For a 3D polycrystal, the relationship between uniaxial strain rate, $\dot{E}^{uniaxial}$, and uniaxial stress, $S^{uniaxial}$, writes

$$\dot{E}^{uniaxial} = \frac{1}{3}\frac{1}{G} S^{uniaxial}. \tag{30}$$

In the case of the periodic lattice model under purely deviatoric loading depicted in Fig. 1, the shear viscosity, *G*, (Eq. (1)) can be derived via

$$G = \frac{\dot{Q}}{4\dot{E}^2} \tag{31}$$

where $\dot{Q}$ denotes the dissipation rate per unit volume, which derives from the dissipations associated to individual GBs as

$$\dot{Q} = \frac{1}{2}\frac{1}{6\sqrt{3}B^2L}\sum_{f=1}^{6}\dot{W}_f . \tag{32}$$

Adding the different contributions to dissipation, we may distinguish seven contributions to *G*:

$$G = G^{diffNH} + G^{diffCoble} + G_{cl}^{pile-up} + G^{\eta} + G^{GBmobility} + G_{cl}^{isol} + G_{gl}^{isol} . \tag{33}$$

These contributions are detailed in subsections 3.1 to 3.5. The main features are summarized in Table 1 for the case of Coble creep.

Table 1: Contributions to shear viscosity (Coble creep)

Dissipation source	**Hexagonal lattice model**	**Relative contribution**
Diffusion fluxes	$G^{diffCoble} = \frac{1}{2\sqrt{3}}\frac{kTB^3}{\delta D_{gbl}}$	
Nucleation and recovery of climbing pile-ups	$G_{cl}^{pile-up} = \frac{1}{4\sqrt{3}}\frac{kTB^3}{\delta D_{gbl}}$	$\frac{G_{cl}^{pile-up}}{G^{diff}} = 0.5$
GB sliding resistance	$G^{\eta} = \frac{\sqrt{3}}{2}\eta B$	$\frac{G^{\eta}}{G^{diffCoble}} \le 0.1$
GB migration resistance	$G^{GBmobility} = \frac{3}{8}\sqrt{\frac{3}{2}}\sqrt{\frac{1}{\mathcal{M}}\frac{kT}{\Omega\delta D_{gbl}}}B^2$	$\frac{G^{GBmobility}}{G^{diffCoble}} \le 0.1$
Nucleation and recovery of isolated climbing and sliding disconnections		$\frac{G_{cl}^{isol} + G_{gl}^{isol}}{G^{diff}} = \infty$ below a threshold stress

3.1. G^{diffNH} *and* $G^{diffCoble}$

The simplest models for diffusional creep have assumed that dissipation arises only from diffusion fluxes. The work power dissipated by the diffusion fluxes feeding the climb of the disconnections along one GB, denoted $\dot{W}^{diff}$, can be calculated via Eq (28) as

$$\dot{W}^{diff} = L\int_{-B}^{B} \Delta\dot{u}_n \left(T_n - T_n^{nucl}\right) dx = \frac{2}{3} ALB^3 \Delta\dot{u}_n^2. \tag{34}$$

It can be verified that the same result as Eq. (34) is obtained in the case of Coble creep using

$$\dot{W}^{diffCoble} = L\frac{kT}{\Omega\delta D_{\text{gbl}}}\int_{-B}^{B} j^2 dx \tag{35}$$

whereas, in the case of Nabarro-Herring creep, the same total dissipation for the six GBs is obtained using

$$\sum_{f=1}^{6} \dot{W}_f^{diffNH} = 2L\frac{kT}{\Omega D_{bulk}} \int_{grainsurface} \mathbf{J}\cdot\mathbf{J} dS. \tag{36}$$

The consistency of Eqs (35) and (36) with Eq. (34) (with the proper value for *A*) attests that the solutions comply with mechanical equilibrium. If the contributions to $\dot{E}^{uniaxial}$ due to bulk diffusion and to GB-layer diffusion are additive, Eqs (31), (32), and (34) yield

$$\dot{E}^{uniaxial} = \frac{1}{3}\left(\frac{1}{G^{diffNH}} + \frac{1}{G^{diffCoble}}\right) S^{uniaxial} = \left(1 + \frac{2}{\sqrt{3}}\frac{\delta}{B}\frac{D_{gbl}}{D_{bulk}}\right)\frac{\Omega D_{bulk}}{kTB^2} S^{uniaxial}. \tag{37}$$

According to Eq. (37), quasi-stationary diffusional creep is characterized by a Newtonian viscosity and a grain size sensitivity exponent equal to 2 or 3 when either Nabarro-Herring creep or Coble creep are dominant.

Extensive reference has been made in the literature to relationships similar to Eq. (37), with somewhat different numerical factors depending on the model [3, 5, 26-29]. Experimental validation is affected by the precision of the available data for diffusion coefficients and for average grain size [30]. The discrepancies between experiments and model predictions have

been the subject of debate [31]. The main objections have focused on the stress sensitivity exponent, which is rarely measured to amount to less than 2 [32, 33]. Arzt et al [5] have discussed how a threshold stress and/or a stress exponent larger than 1 can be justified in the framework of the diffusional creep hypotheses by accounting for the roles of solute segregation and of precipitates.

3.2. $G_{cl}^{pile-up}$

Comparison of Eqs. (26) and (34) shows that $\dot{W}_{cl}^{pile-up}$ amounts to 50% of the dissipation arising from diffusion fluxes. It follows that $G_{cl}^{pile-up} = \frac{G^{diff}}{2}$. The account of the nucleation of climbing pile-ups thus affects neither the stress exponent nor the grain size exponent predicted by the classical model. Experimental validation of the effectiveness of the correction to be brought to Eq. (37) and the like would however be difficult owing to the lack of precision on diffusion coefficients and average grain size. Nevertheless, the correction by a factor 3/2 deserves to be considered in the choice of the value of parameter *G* in numerical simulations of diffusional deformation processes.

We think that, in addition to an increase of *G*, the work spent for the nucleation of climbing pile-ups may significantly contribute to a non-Newtonian behaviour. Indeed, Eq. (24) assumes that the crystals remain purely linear elastic in the close vicinity of TJs regardless of the magnitude of the strain energy density (the strain energy density per unit surface area varies as x^5). It may be anticipated that such a high strain energy density hardly accumulates without the simultaneous nucleation of dislocations emitted from TJs toward the bulk of the lattices. At steady-state, the balance between nucleation and recovery processes can bring these redundant dislocations to form a stationary dislocation forest that remains localized around TJs.

The stress dependence of the dissipation due to these redundant dislocations may be expected to be very non-linear. Such dislocations would not contribute to macroscopic deformation, except perhaps during the primary stage of creep, when the traction offsets at TJs have not yet relaxed to their stationary value T_n^{nucl} (Eq.(27).

3.3. G^{η}

Based on Eq. (29), the dissipation $\dot{W}^{\eta}$ arising from the intrinsic grain boundary viscosity, i.e. from the Peierls barriers opposing disconnection glide, is

$$\dot{W}^{\eta} = L\int_{-B}^{B} \Delta\dot{u}_{//} T_{//} dx = 2BL\eta\Delta\dot{u}_{//}^2. \tag{38}$$

Via Eqs (31) and (32), the contribution to shear viscosity is thus

$$G^{\eta} = \frac{\sqrt{3}}{2}\eta B. \tag{39}$$

G^{η} is linear with grain size. Owing to the lack of experimental method giving access to the phenomenon of GB sliding at grain scale, very little data can be found in the literature to validate the value to be ascribed to η. The relative contribution to *G* due to GB viscosity is commonly expressed via a non-dimensional parameter, $\tilde{\eta}$, defined, in the case of Coble creep for example, as

$$\frac{G^{\eta}}{G^{diffCoble}} = 3\frac{\eta\Omega\delta D_{gbl}}{kTB^2} = 3\tilde{\eta}. \tag{40}$$

Although a large range of $\tilde{\eta}$ values have been considered in the literature, it is most widely admitted that $0 \le \tilde{\eta} \le 0.1$ [19, 34-36].

3.4. $G^{GBmobility}$

The role of GB mobility in diffusional deformation has been analysed recently by the present author [37]. GB migration is a necessary ingredient in the diffusional deformation mechanism because GB curvature is a condition for the transfer of diffusion fluxes across grain boundaries. The dissipations due both to GB migration and to diffusion fluxes driven by curvature gradients translate into a contribution to *G*, denoted $G^{GBmobility}$, that can be written

$$G^{GBmobility} = \frac{3}{8}\sqrt{\frac{3}{2}}\sqrt{\frac{1}{\mathcal{M}}\frac{kT}{\Omega\delta D_{gbl}}}B^2 \tag{41}$$

where $\mathcal{M}$ denotes the GB mobility. With respect to $G^{diffCoble}$, Eq. (41) brings

$$\frac{G^{GBmobility}}{G^{diffCoble}} = \frac{9}{4\sqrt{2}}\sqrt{\frac{1}{\mathcal{M}}\frac{\Omega\delta D_b}{kT}}\frac{1}{B}. \tag{42}$$

According to the values for $\mathcal{M}$ and δD_b that can be retrieved in the literature, $\sqrt{\frac{1}{\mathcal{M}}\frac{\Omega\delta D_b}{kT}}$ varies between 1 nm and 50 nm [37]. It follows that, $10^{-5} \le \frac{G^{GBmobility}}{G^{diffCoble}} \le 0.1$. The weights of $G^{GBmobility}$ and G^{η} are thus comparable.

3.5. $G_{cl}^{isol} + G_{gl}^{isol}$

Climbing and sliding disconnections contribute together to an additional dissipation, $\dot{W}_{cl}^{isol} + \dot{W}_{gl}^{isol}$, which increases linearly with $\dot{E}$ (Eq. (9)) in contrast to the other dissipation sources which increase as $\dot{E}^2$. It follows that $G_{cl}^{isol} + G_{gl}^{isol}$ increases when strain rate decreases and is infinite below a threshold stress, $S_{threshold}^{uniaxial}$, which increases when grain size decreases: taking $G_{cl}^{isol} = G_{gl}^{isol}$ and $\dot{E}^{uniaxial} = 2\dot{E}_{i\neq j}$, one obtains via Eqs. (5), (6), (9) (30), (31), and (32)

$$S_{threshold}^{uniaxial} = \frac{1}{8\pi}\frac{\mu}{1-\nu}\frac{|b|}{B}\ln\left(\frac{B}{2|b|}\right)\sum_{f=1}^{6}\left|\cos\left(2\alpha - 2f\frac{\pi}{3}\right)\right|. \quad (43)$$

As a corollary, the stress exponent increases sharply when $S^{uniaxial}$ decreases toward $S_{threshold}^{uniaxial}$.

The existence of a threshold stress for diffusional creep in pure polycrystals was pointed out by Burton [10] and by Arzt et al [5]. These authors linked the threshold to the energy barrier to be overcome for the bowing of the GB dislocations climbing on the grain surface: the critical bowing radius being proportional to grain size, the threshold should scale as the inverse of grain size. In the present work, the threshold is linked to the work needed to maintain the balance between nucleation and recovery for isolated, non-interacting disconnections moving by climbing and gliding. In Figure 4, the continuous red line represents on a log-log graph the variation of $S_{threshold}^{uniaxial}$ averaged over α according to Eq. (43) as a function of the average grain diameter defined as $2R_G = 1.82\,B$, with Poisson's ratio taken $\nu = 1/3$. The dashed line displays the relationship $S_{threshold}^{uniaxial} = \frac{1}{2}\frac{b}{2R_G}\mu$ used by Arzt et al for assessing the correspondence with a set of experimental data reported in the literature for the threshold stress in pure metals [5]. The curve calculated via Eq. (43) is larger than the dashed line by a factor comprised between 10 to 20. The difference amounts essentially to the factor $\ln\left(\frac{B}{2|b|}\right)$. Actually, Eq. (9) represents an upper bound for $\dot{W}^{isol}$ because, in order to account for the presence of the geometrical disconnections, factor $\ln\left(\frac{B}{2|b|}\right)$ should be substituted by $\ln\left(\frac{1}{2\rho_{geom}|b|}\right)$ where ρ_{geom} is the density of geometrical disconnections. A more precise assessment of the curves in Fig. 4 is not possible owing to the large scatter of the available experimental data for the

threshold stress in pure polycrystals and to the uncertainty about the value to be ascribed (i) to the average Burgers vector of moving disconnections, $|b|$, and (ii) to the geometrical disconnection density, ρ_{geom}. Most importantly, Eq. (43) emphasizes the fact that the existence of a threshold stress is an intrinsic feature which should not be overlooked in the analyses of the processes of sintering or superplastic forming based on the postulates of the diffusional deformation model.

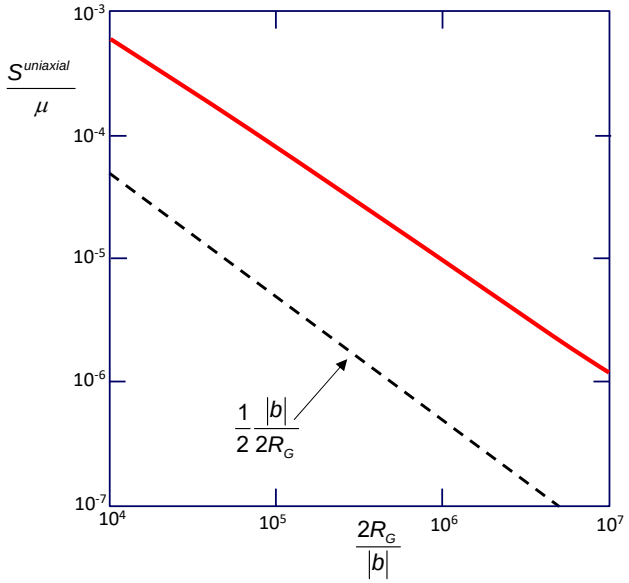

Figure 5: Variation of the stress threshold $S^{uniaxial}_{threshold}$ as a function of the average grain size according to Eq. (43). The dashed line is the relationship proposed by Arzt et al [5].

4. Conclusion

The main outcomes can be summarized as follows.

- Static equilibrium along grain boundaries implies a parabolic distribution of the density of climbing disconnections during straining.

- The work of nucleation of climbing disconnections brings an increase by 50% of the macroscopic viscosity with respect to the prediction of models accounting only for diffusion fluxes. This correction deserves to be implemented in the simulation of diffusional deformation processes.
- The high strain energy to be built in the vicinity of triple junctions for the onset of nucleation may be the source of non-Newtonian behaviour.
- The analysis emphasizes the fact that the existence of a threshold stress is intrinsic to the diffusional deformation mechanism. The threshold stress is contributed by the work of nucleation of both sliding and climbing disconnections.

Acknowledgements

This research did not receive any specific grant from funding agencies in the public, commercial, or not-for-profit sectors.

References

[1] F.R.N. Nabarro. Deformation of crystals by the motion of single ions. Conference on Strength of Solids. Bristol: Physical Society London, 1948. p.75-90.
[2] C. Herring. Diffusional Viscosity of a Polycrystalline Solid, J Appl Phys 21 (1950) 437-445.
[3] R. Raj, M.F. Ashby. On grain boundary sliding and diffusional creep, Metallurgical transactions 2 (1971) 1113-1127.
[4] M. Ashby. Boundary defects, and atomistic aspects of boundary sliding and diffusional creep, Surface Science 31 (1972) 498-542.
[5] E. Arzt, M.F. Ashby, R.A. Verrall. Interface controlled diffusional creep, Acta Metallurgica 31 (1983) 1977-1989.
[6] I. Lifshitz. On the theory of diffusion-viscous flow of polycrystalline bodies, Soviet Physics JETP 17 (1963) 909-920.

[7] Y. Ishida, M.H. Brown. Dislocations in grain boundaries and grain boundary sliding, Acta Metallurgica 15 (1967) 857-860.
[8] H. Gleiter, E. Hornbogen, G. Baro. The mechanism of grain boundary glide, Acta Metallurgica 16 (1968) 1053-1067.
[9] M.F. Ashby. On interface-reaction control of Nabarro-Herring creep and sintering, Scripta Metallurgica 3 (1969) 837-842.
[10] B. Burton. Interface reaction controlled diffusional creep: a consideration of grain boundary dislocation climb sources, Materials Science and Engineering 10 (1972) 9-14.
[11] J.P. Hirth. Dislocations, steps and disconnections at interfaces, Journal of Physics and Chemistry of Solids 55 (1994) 985-989.
[12] J.P. Hirth, R.C. Pond. Steps, dislocations and disconnections as interface defects relating to structure and phase transformations, Acta Materialia 44 (1996) 4749-4763.
[13] J.P. Hirth, J. Wang, C.N. Tomé. Disconnections and other defects associated with twin interfaces, Progress in Materials Science 83 (2016) 417-471.
[14] J. Han, S.L. Thomas, D.J. Srolovitz. Grain-boundary kinetics: A unified approach, Progress in Materials Science 98 (2018) 386-476.
[15] R.W. Balluffi, S. Allen, W.C. Carter. Kinetics of materials, John Wiley & Sons, 2005.
[16] A.H. Heuer, M. Zahiri Azar. A disconnection mechanism of enhanced grain boundary diffusion in Al2O3, Scripta Materialia 102 (2015) 15-18.
[17] J.C. Fisher. Calculation of Diffusion Penetration Curves for Surface and Grain Boundary Diffusion, J Appl Phys 22 (1951) 74-77.
[18] F. Delannay. The role of grain boundary mobility in diffusional deformation Journal of the Mechanics and Physics of Solids in press (2021).
[19] F. Delannay, L. Brassart. Variational analysis of the influence of grain shape anisotropy on shear viscosity in Nabarro-Herring-Coble creep, Mech Mater 143 (2020) 103312.
[20] J. Spingarn, W. Nix. Diffusional creep and diffusionally accommodated grain rearrangement, Acta Metallurgica 26 (1978) 1389-1398.
[21] B.-N. Kim, K. Hiraga, K. Morita, B.-W. Ahn. Analysis of creep due to grain-boundary diffusion in hexagonal microstructures, Philosophical Magazine 84 (2004) 3251-3262.
[22] J.F. Rudge. The Viscosities of Partially Molten Materials Undergoing Diffusion Creep, Journal of Geophysical Research: Solid Earth 123 (2018) 10,534-510,562.
[23] P.M. Anderson, J.P. Hirth, J. Lothe. Theory of dislocations, Cambridge University Press, 2017.
[24] W. Beere. Stresses and Deformation at Grain Boundaries [and Discussion], Philosophical Transactions of the Royal Society of London A: Mathematical, Physical and Engineering Sciences 288 (1978) 177-196.
[25] J.P. Hirth, G. Hirth, J. Wang. Disclinations and disconnections in minerals and metals, Proceedings of the National Academy of Sciences 117 (2020) 196-204.
[26] B.-N. Kim, K. Hiraga. Simulation of diffusional creep accompanied by grain growth in two-dimensional polycrystalline solids, Acta materialia 48 (2000) 4151-4159.
[27] B.-N. Kim, K. Hiraga, K. Morita, I.-W. Chen. Rate of creep due to grain-boundary diffusion in polycrystalline solids with grain-size distribution, Philosophical Magazine 85 (2005) 2281-2292.
[28] S. Shah, A.H. Chokshi. The significance of diffusional flow in ultrafine-grained materials, Colloids and Surfaces A: Physicochemical and Engineering Aspects 133 (1998) 57-61.
[29] H.S. Kim, Y. Estrin, M.B. Bush. Plastic deformation behaviour of fine-grained materials, Acta Materialia 48 (2000) 493-504.

[30] A.H. Chokshi. Diffusion creep in metals and ceramics: Extension to nanocrystals, Materials Science and Engineering: A 483-484 (2008) 485-491.
[31] B. Burton, G.L. Reynolds. In defense of diffusional creep, Materials Science and Engineering: A 191 (1995) 135-141.
[32] T.G. Langdon. A unified approach to grain boundary sliding in creep and superplasticity, Acta Metallurgica et Materialia 42 (1994) 2437-2443.
[33] O.A. Ruano, J. Wadsworth, O.D. Sherby. Deformation of fine-grained alumina by grain boundary sliding accommodated by slip, Acta Materialia 51 (2003) 3617-3634.
[34] F. Wakai, Z.S. Nikolić. Effect of grain boundary sliding on shear viscosity and viscous Poisson's ratio in macroscopic shrinkage during sintering, Acta Materialia 59 (2011) 774-784.
[35] L. Brassart, F. Delannay. Bounds for shear viscosity in Nabarro–Herring–Coble creep, Mech Mater 137 (2019) 103106.
[36] B. Henrich, A. Wonisch, T. Kraft, M. Moseler, H. Riedel. Simulations of the influence of rearrangement during sintering, Acta Materialia 55 (2007) 753-762.
[37] F. Delannay. The role of grain boundary mobility in diffusional deformation, Journal of the Mechanics and Physics of Solids 154 (2021) 104512.